Fig. 5 Influence of CCT5, YKT6, and RGS3-specific siRNA on docetaxel-induced apoptosis in MCF-7 cells. MCF-7 cells were transfected with iCCT5, iYKT6, or iRGS3 alone and treated with 10 nM docetaxel for 24 h. Cells were then analyzed in apoptosis using the TUNEL assay. The percentages of apoptotic cells in each sample are shown. Bars: mean ± SD of triplicate determinations (P; * <0.05, and ** <0.01)

not significant. Our present observations seem to suggest that p53 mutations might play a certain role in resistance to docetaxel though a significant association has failed to be demonstrated probably due to the limited number of breast tumors ($n = 50$) analyzed in the present study.

We attempted to select the genes, which were differentially expressed between p53-wild and p53-mutated breast tumors by ATAC-PCR since such genes were speculated to play some role in resistance to docetaxel. DNA microarrays have a wider coverage of genes than ATAC-PCR but genes with low expression are excluded from the analysis with DNA microarrays. On the other hand, ATAC-PCR can be used to measure expression of the genes with low expression. In addition, ATAC-PCR requires a very small amount of RNA and can tolerate RNA degradation to some extent because this technique only uses the 3′ end of cDNA or mRNA. Actually, we have successfully applied ATAC-PCR to the study on gene expression profiling of breast cancers [28], thyroid cancers [29], hepatocellular carcinomas [30], gastric cancers [31], and colon cancers. In the present study, we have applied ATAC-PCR to the identification of genes differentially expressed between p53-wild and p53-muated breast tumors, and have found that mRNA expression of the 13 genes is significantly different (Table 4). Then, we studied the relationship of the mRNA expression of these 13 genes with response to docetaxel, where a real-

time PCR assay was employed instead of ATAC-PCR because a real-time PCR is currently considered to be the most reliable method for quantification of mRNA levels. Eventually, we found that mRNA levels of three genes, i.e., CCT5, RGS3, and YKT6, were significantly associated with resistance to docetaxel. For the purpose of confirming the involvement of these three genes in resistance to docetaxel, we conducted a study with siRNA designed for knocking down of these genes. We were able to shown that siRNA treatment for each of these genes resulted in enhancement of docetaxel-induced apoptosis in MCF-7 cells, indicating that these genes play a significant role in resistance to docetaxel though the precise mechanism of action of these genes still remains to be studied.

Little is known about CCT5, RGS3, and YKT6 in breast cancer biology, and, at least, their mRNA expression is unlikely to be regulated directly by p53 because promoter regions of these three genes seem to lack the typical consensus sequence for p53 binding. Rather, they are likely to represent downstream effectors modulated by functional induction of p53 in the orchestration of apoptosis and tumor suppression. CCT5 is a molecular chaperone and is a member of the chaperonin containing TCP1 complex (CCT), also known as the TCP1 ring complex (TRiC). Unfolded polypeptides enter the central cavity of this complex and are folded in an ATP-dependent manner. The complex folds the various proteins including the β-tubulin. Microtubule cytoskeleton perturbation induced by paclitaxel is reported to increase CCT5 expression in *Tetrahymena* cells [32]. We also found an increase in CCT5 protein after docetaxel treatment. An increased expression of CCT5 is seen in multidrug-resistant gastric carcinoma cells [33]. Taken together with our present observation that treatment with CCT5-specific siRNA resulted in enhancement of docetaxel-induced apoptosis, it is suggested that CCT5 is involved in resistance to docetaxel though its mechanism still remains to be studied. RGS3 is a member of regulators of G-protein signaling (RGS) family that accelerates the intrinsic GTPase activity of G-alpha subunit. RGS3 regulates cellular adhesive and migratory behaviors [34]. Recently, expression of RGS3 was shown to be up-regulated in glioma cells and to enhance both adhesion and migration [35]. RGS3 interacts with ERα transcriptional activities [36], raising the possibility that RGS3 might be involved in the growth of breast cancer. Role of RGS3 in resistance to chemotherapy including docetaxel has never been reported. YKT6 is one of the soluble N-ethylmaleimide-sensitive factor attachment protein receptor (SNARE) recognition molecules implicated in vesicular transport between

secretory compartments. It is a membrane associated, isoprenylated protein that functions at the endoplasmic reticulum–Golgi transport step. YKT6 is expressed at high levels in brain neurons. However, recently, YKT6 has been showed to be expressed in breast cancers and associated with invasive phenotypes [37], suggesting a possible involvement of this molecule in the pathogenesis and progression of breast cancer. Role of YKT6 in resistance to chemotherapy has never been reported.

In conclusion, we have shown that CCT5, RGS3, and YKT6 mRNA expression are up-regulated in p53-mutated breast tumors and are associated with a resistance to docetaxel. We have been able to further substantiate the implication of these genes through studies with siRNA. Our present observation seems to suggest that these genes might be clinically useful in identifying the subset of breast cancer patients who may or may not benefit from docetaxel treatment. Furthermore, our results might provide a new insight into research for molecular mechanism of resistance to docetaxel.

References

1. Piccart MJ, de Valeriola D, Dal Lago L et al (2005) Adjuvant chemotherapy in 2005: standards and beyond. Breast 14:439–445
2. Hudis C (2005) The best use of adjuvant chemotherapy: new drugs and new use of "old" drugs. Breast 14:570–575
3. Charfare H, Limongelli S, Purushotham AD (2005) Neoadjuvant chemotherapy in breast cancer. Br J Surg 92:14–23
4. Trudeau M, Sinclair SE, Clemons M, Breast Cancer Disease Site Group (2005) Neoadjuvant taxanes in the treatment of non-metastatic breast cancer: a systematic review. Cancer Treat Rev 31:283–302
5. O'Shaughnessy J (2005) Extending survival with chemotherapy in metastatic breast cancer. Oncologist 10(Suppl 3): 20–29
6. Mauriac L, Debled M, MacGrogan G (2005) When will more useful predictive factors be ready for use? Breast 14:617–623
7. Sjostrom J, Blomqvist C, Heikkila P et al (2000) Predictive value of p53, mdm-2, p21, and mib-1 for chemotherapy response in advanced breast cancer. Clin Cancer Res 6:3103–3110
8. Palmeri S, Vaglica M, Spada S et al (2005) Weekly docetaxel and gemcitabine as first-line treatment for metastatic breast cancer: results of a multicenter phase II study. Oncology 68(4–6):438–445
9. Figgitt DP, Wiseman LR (2000) Docetaxel: an update of its use in advanced breast cancer. Drugs 59:621–651
10. Sjostrom J, Blomqvist C, von Boguslawski K et al (2002) The predictive value of bcl-2, bax, bcl-xL, bag-1, fas, and fasL for chemotherapy response in advanced breast cancer. Clin Cancer Res 8:811–816

11. Buchholz TA, Davis DW, McConkey DJ et al (2003) Chemotherapy-induced apoptosis and Bcl-2 levels correlate with breast cancer response to chemotherapy. Cancer J 9:33–41
12. Miyoshi Y, Taguchi T, Kim SJ et al (2005) Prediction of response to docetaxel by immunohistochemical analysis of CYP3A4 expression in human breast cancers. Breast Cancer 12:11–15
13. Shalli K, Brown I, Heys SD, Schofield AC (2005) Alterations of beta-tubulin isotypes in breast cancer cells resistant to docetaxel. FASEB J 19:1299–1301
14. Egawa C, Miyoshi Y, Takamura Y et al (2001) Decreased expression of BRCA2 mRNA predicts favorable response to docetaxel in breast cancer. Int J Cancer 95:255–259
15. Im SA, Kim SB, Lee MH et al (2005) Docetaxel plus epirubicin as first-line chemotherapy in MBC (KCSG 01-10-05): phase II trial and the predictive values of circulating HER2 extracellular domain and vascular endothelial growth factor. Oncol Rep 14:481–487
16. Rouzier R, Rajan R, Wagner P et al (2005) Microtubule-associated protein tau: a marker of paclitaxel sensitivity in breast cancer. Proc Natl Acad Sci USA 102:8315–8320
17. Chang JC, Wooten EC, Tsimelzon A et al (2005) Patterns of resistance and incomplete response to docetaxel by gene expression profiling in breast cancer patients. J Clin Oncol 23:1169–1177
18. Iwao-Koizumi K, Matoba R, Ueno N et al (2005) Prediction of docetaxel response in human breast cancer by gene expression profiling. J Clin Oncol 23:422–431
19. Learn PA, Yeh IT, McNutt M et al (2005) HER-2/neu expression as a predictor of response to neoadjuvant docetaxel in patients with operable breast carcinoma. Cancer 103:2252–2260
20. Bergh J, Norberg T, Sjogren S, Lindgren A, Holmberg L (1995) Complete sequencing of the p53 gene provides prognostic information in breast cancer patients, particularly in relation to adjuvant systemic therapy and radiotherapy. Nat Med 1:1029–1034
21. Aas T, Borresen AL, Geisler S et al (1996) Specific P53 mutations are associated with de novo resistance to doxorubicin in breast cancer patients. Nat Med 2:811–814
22. Wurzburger RJ, Gupta R, Parnassa AP et al (2003) Use of GC clamps in DHPLC mutation scanning. Clin Med Res 1:111–118
23. Zhang L, Jia G, Li WM, Guo RF, Cui JT, Yang L, Lu YY (2004) Alteration of the ATM gene occurs in gastric cancer cell lines and primary tumors associated with cellular response to DNA damage. Mutat Res 557:41–51
24. Saito S, Matoba R, Kato K (2003) Adapter-tagged competitive PCR (ATAC-PCR) – a high-throughput quantitative PCR method for microarray validation. Methods 31:326–331
25. Elbashir SM, Harborth J, Weber K, Tuschl T et al (2002) Analysis of gene function in somatic mammalian cells using small interfering RNAs. Methods 26:199–213
26. Andersson J, Larsson L, Klaar S et al (2005) Worse survival for TP53 (p53)-mutated breast cancer patients receiving adjuvant CMF. Ann Oncol 16:743–748
27. Soussi T, Beroud C (2001) Assessing TP53 status in human tumours to evaluate clinical outcome. Nat Rev Cancer 1:233–240
28. Iwao K, Matoba R, Ueno N et al (2002) Molecular classification of primary breast tumors possessing distinct prognostic properties. Hum Mol Genet 11:199–206

29. Taniguchi K, Takano T, Miyauchi A et al (2005) Differentiation of follicular thyroid adenoma from carcinoma by means of gene expression profiling with adapter-tagged competitive polymerase chain reaction. Oncology 69:428–435

30. Kurokawa Y, Matoba R, Nakamori S et al (2004) PCR-array gene expression profiling of hepatocellular carcinoma. J Exp Clin Cancer Res 23:135–141

31. Motoori M, Takemasa I, Yano M et al (2005) Prediction of recurrence in advanced gastric cancer patients after curative resection by gene expression profiling. Int J Cancer 114:963–968

32. Casalou C, Cyrne L, Rosa MR, Soares H (2001) Microtubule cytoskeleton perturbation induced by taxol and colchicine affects chaperonin containing TCP-1 (CCT) subunit gene expression in Tetrahymena cells. Biochim Biophys Acta 1522:9–21

33. Ludwig A, Dietel M, Lage H (2002) Identification of differentially expressed genes in classical and atypical multidrug-resistant gastric carcinoma cells. Anticancer Res 22:3213–3221

34. Bowman EP, Campbell JJ, Druey KM, Scheschonka A, Kehrl JH, Butcher EC (1998) Regulation of chemotactic and proadhesive responses to chemoattractant receptors by RGS (regulator of G-protein signaling) family members. J Biol Chem 273:28040–28048

35. Tatenhorst L, Senner V, Puttmann S, Paulus W (2004) Regulators of G-protein signaling 3 and 4 (RGS3, RGS4) are associated with glioma cell motility. J Neuropathol Exp Neurol 63:210–222

36. Ikeda M, Hirokawa M, Satani N (2001) Molecular cloning and characterization of a steroid receptor-binding regulator of G-protein signaling protein cDNA. Gene 273:207–214

37. Kluger HM, Kluger Y, Gilmore-Hebert M et al (2004) cDNA microarray analysis of invasive and tumorigenic phenotypes in a breast cancer model. Lab Invest 84:320–331

ELSEVIER

CANCER
Letters

Demonstration of *Adiponectin Receptors 1* and *2* mRNA expression in human breast cancer cells

Chie Takahata [a,b], Yasuo Miyoshi [a], Natsumi Irahara [a], Tetsuya Taguchi [a],
Yasuhiro Tamaki [a], Shinzaburo Noguchi [a,*]

[a] *Department of Breast and Endocrine Surgery, Osaka University Graduate School of Medicine, Osaka, Japan*
[b] *Faculty of Health Sciences, Kobe University Graduate School of Medicine, Hyogo, Japan*

Abstract

Recently, we have shown that low adiponectin levels are significantly associated with an increased breast cancer risk. It seems to be very important to study the expression of adiponectin receptor 1 (AdipoR1) and receptor 2 (AdipoR2) in the human breast epithelial cells and breast cancer cells in order to clarify whether or not adiponectin exerts its effects directly on these cells. Expression of *adiponectin, AdipoR1*, and *AdipoR2* mRNA was determined by RT-PCR assay using the RNA samples obtained from human breast cancer cell lines (MCF-7, T47D, SKBR3, and MDA-MB231), HMEC (primary culture of normal human mammary epithelial cells), adipose tissues (axilla) as well as breast cancer cells and normal breast epithelial cells selectively collected from breast cancer tissues by laser microdissection (LMD). *Adiponectin* mRNA expression was observed only in the adipose tissues. On the other hand, *AdipoR1* and *AdipoR2* mRNA expression was observed in all four breast cancer cell lines, HMEC, adipose tissues as well as breast cancer cells and normal breast epithelial cells selectively collected by LMD. In addition, AdipoR1 and AdipoR2 expression in both normal breast epithelial cells and breast cancer cells was confirmed by immunohistochemistry. These results suggest a possibility that adiponectin might modulate the growth of normal breast epithelial cells and breast cancer cells directly through AdipoR1 and AdipoR2 receptors, and that the association of low serum adiponectin levels with a high breast cancer risk might be explained, at least in part, by the direct effect of adiponectin on the breast epithelial cells.
© 2006 Elsevier Ireland Ltd. All rights reserved.

Keywords: Breast cancer; Adiponectin; Adiponectin receptor; Laser microdissection

1. Introduction

It is well established that body mass index (BMI) is associated with an increase risk of breast cancer,

* Corresponding author. Tel.: +81 6 6879 3772; fax: +81 6 6879 3779.
E-mail address: noguchi@onsurg.med.osaka-u.ac.jp (S. Noguchi).

especially in postmenopausal women [1,2]. This association seems to be partially explained by the higher serum estrogens levels seen in postmenopausal women with high BMI as compared with those with low BMI since serum estrogens levels have been repeatedly shown to be significantly associated with breast cancer risk [3–9]. However, the fact that BMI is associated with breast cancer risk even after

the adjustment of serum estrogens levels indicates that high BMI affects the breast cancer risk through other mechanism [3,9].

Recent studies have disclosed that the adipose tissue is not merely a fat-storing tissue but also an endocrine organ producing various cytokines including adiponectin. Adiponectin is a peptide hormone secreted from only the adipose tissue, and it belongs to the collectin family [10,11]. This peptide has been shown to play a preventive role in the pathogenesis of atherosclerosis through the inhibition of vascular smooth muscle and endothelial cell proliferation [12,13] and in the pathogenesis of diabetes through the modulation of glucose and fatty acid metabolism and insulin sensitivity in various stromal and epithelial cells [14–17]. Very recently, we have shown that low adiponectin levels are significantly associated with an increased risk of breast cancer [18], and our finding was later confirmed by Mantzoros et al. [19]. In addition, it has been reported that adiponectin levels are inversely related to the risk of endometrial cancer [20]. Interestingly, it is well established that obesity is associated with an increased risk of endometrial cancer in analogy to breast cancer [21].

Recently, receptors for adiponectin, receptor 1 (AdipoR1) and 2 (AdipoR2), have been identified [22]. In mice, AdipoR1 is expressed in the various organs such as skeletal muscle, lung, and spleen [22] and AdipoR2 is predominantly expressed in the liver [22]. In humans, expression of AdipoR1 and AdipoR2 have been reported in the islet cells of the pancreas [23], macrophages [24], adipocytes [25], and vascular smooth muscle [24] but it has not been studied yet whether these receptors are expressed in the human breast epithelial cells and breast cancer cells. Since adiponectin exerts its effects through these receptors, it is very important to investigate the presence or absence of their expression in these cells in order to prove the possible direct effect of adiponectin. Therefore, in the present study, we have studied the *AdipoR1* and *AdipoR2* mRNA expression in human breast cancer cell lines as well as in human breast epithelial cells and breast cancer cells selectively obtained using the laser microdissection technique. Furthermore, immunohistochemical staining was also investigated for AdipoR1 and AdipoR2 in normal breast epithelial cells and breast cancer cells.

2. Materials and methods

2.1. Breast tumor tissues and non-tumor tissues

Tumor tissues, non-tumor breast tissues, and axillary adipose tissues were obtained at surgery from female primary breast cancer patients (Stages I–III between December 2000 and May 2003). The median age of the patients was 54.8 years (range, 30–83 years). The specimens were snap-frozen in liquid nitrogen and kept at −80 °C until use. Several tumor specimens and non-tumor specimens were embedded in the Tissue-Tek OCT compound (SAKURA Finetechnical, Tokyo, Japan) to be used for laser microdissection (LMD). Informed consent as to this study was obtained from each patient before surgery.

2.2. Breast cancer cell lines and normal human mammary epithelial cells (HMEC)

MCF-7 and MDA-MB-231 cells were cultured in Dulbecco's modified Eagle's medium (Nihonseiyaku, Tokyo, Japan) supplemented with 10% fetal calf serum (Dainippon Pharmaceutical, Tokyo, Japan), 500 U/ml penicillin (Gibco BRL, MD, USA), and 500 μg/ml streptomycin (Gibco BRL, MD, USA) in a 5% CO_2 incubator at 37 °C. T-47D cells were cultured in RPMI 1640 (Nissui, Pharm., Tokyo, Japan), SK-BR-3 cells were cultured in McCoy5a (Gibco BRL, MD, USA) with the same supplement. HMECs were purchased from Cambrex Bio Science Walkersville (Whittaker, USA) and the culture was done according to the manufacturer's protocol.

2.3. RNA extraction

Total cellular RNA was extracted from the tumor specimens and cultured cells using TRIZOL reagent according to the protocol provided by the manufacturer (Molecular Research Center, Cincinnati, OH).

2.4. Laser microdissection

Frozen tissue samples embedded in Tissue-Tek OCT compound (SAKURA Finetechnical, Tokyo, Japan) were cut into 8-μm sections in a cryostat. The sections were stained with toluidine blue (Muto Pure Chemicals, Tokyo, Japan), and tumor cells and normal epithelial cells were collected with Application Solutions Laser Microdissection System (Leica Microsystems, Wetzler, Germany) according to the manufacturer's protocol. The total RNA was extracted from microdissected cells using RNeasy Micro Kit according to the protocol provided by the manufacturer (Qiagen, Hilden, Germany).

2.5. Semi-quantitative reverse transcription-polymerase chain reaction (RT-PCR) assay of adiponectin, AdipoR1, and AdipoR2 mRNA expression

The 3 µg of total RNA underwent RT for single strand cDNA using oligo(dT)$_{15}$ primer and Superscript II (Life Technologies, Inc., Bethesda, MD) and were scaled up to a final volume of 50 µl. The RT reaction was performed at 42 °C for 50 min, followed by heating at 70 °C for 15 min.

Primer pairs for the amplification of adiponectin, AdipoR1, and AdipoR2 mRNA were selected so that they were located at different exons to prevent amplification from the contaminated genomic DNA. Quantitative normalization of cDNA in each sample was performed using expression of the β-glucuronidase gene as an internal control. In humans, primer sequences were 5′-CAGGCC GTGATGGCAGAGAT-3′ and 5′-AGTCTCCAATCCC ACACTGAAT-3′ for adiponectin, 5′-AATTCCTGAG CGCTTCTTTCCT-3′ and 5′-CATAGAAGTGGACAA AGGCTGC-3′ for AdipoR1, 5′-TGCAGCCATTATAG TCTCCCAG-3′ and 5′-GAATGATTCCACTCAGGCC TAG-3′ for AdipoR2, 5′-ATTGCAGGGTTTCACCA GGA-3′ and 5′-GTCGGTGACTGTTCAGTCATGAA-3′ for β-glucuronidase. The PCR condition for adiponectin and AdipoR1 was established as follows: after denaturing at 96 °C for 5 min, 37 cycles of 96 °C for 30 s, 60 °C for 30 s, and 72 °C for 30 s, and that for AdipoR2 was established as follows: after denaturing at 96 °C for 5 min, 45 cycles of 96 °C for 30 s, 54 °C for 30 s, and 72 °C for 30 s.

2.6. Primers, probes, and real-time PCR

Real-time PCR assays of AdipoR1 and AdipoR2 mRNA expression levels were performed using the ABI Prism 7700/7900 Sequence Detection System (Perkin-Elmer Applied Biosystems, Foster City, CA). The standard curves for AdipoR1 and AdipoR2 mRNA expression were generated using serially diluted solutions of each PCR product as template. The amount of target gene expression was calculated from the standard curve, and quantitative normalization of cDNA in each sample was performed using expression of the β-glucuronidase gene as an internal control. Real-time PCR assays were conducted in duplicate for each sample, and a mean value was used for calculation of the mRNA levels.

The sequence of primers for AdipoR1 and AdipoR2 were described above, and probes were 5′-TGACATAT GGTTCCAGTCTCATCA-3′ and 5′-AACACTCCTG CTCTTACTCCCCGATA-3′, respectively. Probes were labeled with FAM as a reporter at the 5′ end and TAM-RA as a quencherdye at the 3′ end. The PCR condition for AdipoR1 was established as follows: after incubation at 50 °C for 2 min and denaturing at 95 °C for 10 min, 45 cycles of 95 °C for 15 s and 62 °C for 30 s, and that for AdipoR2 was established as follows: after incubation at 50 °C for 2 min and denaturing at 95 °C for 10 min, 45 cycles of 95 °C for 15 s and 58 °C for 30 s. The primer probe mixture for the assay of β-glucuronidase mRNA expression levels was purchased from Perkin-Elmer Applied Biosystems (Foster City, CA). Finally, mRNA levels of AdipoR1 and AdipoR2 were shown as ratios to β-glucuronidase mRNA levels when 10^{-12} µg of PCR product for AdipoR1 and AdipoR2, and 10^{-8} µg of PCR product for β-glucuronidase were defined as 1.

2.7. Immunohistochemical staining of AdipoR1 and AdipoR2

Expression of AdipoR1 and AdipoR2 protein in tissue sections was studied by immunohistochemistry. Polyclonal antibodies against human adipoR1 and adipoR2 were purchased from ABR (Golden, CO, USA) and Phoenix Pharmaceuticals (Belmont, CA, USA), respectively. Sections (3 µm) were prepared from formalin fixed paraffin embedded tissue specimens, deparaffinised, and rehydrated in graded alcohols. Antigen retrieval was performed by incubating the sections in target retrieval solution (DAKO, Japan) for 30 min in 95 °C water bath. After quenching endogenous peroxidase with 3% H_2O_2 in phosphate buffered saline for 20 min, slides were incubated with primary antibodies at 4 °C overnight (anti-adipoR1 antibody, 10 µg/ml; anti-adipoR2 antibody, 10 µg/ml), followed by incubating with biotinylated anti-rabbit immunoglobulin G antibody (Jackson ImmunoResearch Laboratories) using the ABC Kit (Vector Laboratories, Burlingame, CA) for AdipoR1, or Histofine (Max-PO (Multi), Nichirei Bioscience, Osaka, Japan) for AdipoR2 at room temperature for 1 h. Then, antibody complex was visualized with the 3,3′-diaminobenzidine tetrahydrochloride (MERCK, Darmstadt, Germany).

2.8. Statistical analysis

Association between the clinicopathological factors and AdipoR1 or AdipoR2 mRNA levels were assessed by the Mann–Whitney test or Kruskal–Wallis test. Statistical significance was assumed for $P < 0.05$.

3. Results

3.1. Adiponectin, AdipoR1, and AdipoR2 mRNA expression

Expression of adiponectin, AdipoR1, and AdipoR2 mRNA was determined by semiquantitative RT-PCR assay using the RNA samples obtained from human breast cancer cell lines (MCF-7, T47D, SKBR3, and MDA-MB231), HMEC, adipose tissues, and LMD samples (breast cancer cells, normal breast epithelial cells, and stromal cells) from breast cancer tissues. Adiponectin mRNA expression was observed in the adipose tissues but

not in any breast cancer cell lines and HMEC as well as LMD samples (Fig. 1). On the other hand, *AdipoR1* mRNA expression was observed in all four breast cancer cell lines, HMEC, and adipose tissues as well as in all cancer cell samples ($n = 6$), normal epithelial cell samples ($n = 2$), and stromal cell samples ($n = 3$) collected by LMD. *AdipoR2* mRNA expression was observed in all four breast cancer cell lines, HMEC, and adipose tissues as well as in five of six cancer cell samples and all normal epithelial cell samples ($n = 2$), but not in one cancer cell sample and all three stromal cell samples collected by LMD (Figs. 2 and 3).

3.2. AdipoR1 and AdipoR2 protein expression by immunohistochemistry

Protein expression of AdipoR1 and AdipoR2 in normal breast epithelial cells and breast cancer cells was studied in representative cases. As shown in Fig. 4, membranous and cytoplasmic staining of AdipoR1 and AdipoR2 was recognized both in normal breast epithelial cells and breast cancer cells. AdipoR1, but not AdipoR2, expression was also observed in stromal cells.

3.3. Relationship between AdipoR1 or AdipoR2 mRNA levels and clinicopathological characteristics of breast cancers

AdiopR1 and *AdipoR2* mRNA levels were determined by a real-time PCR assay and their expression levels were compared with various clinicopathological characteristics of breast cancers including menopausal status, tumor size, lymph node status, histological grade, and estrogen receptor (ER) status. There was no significant association between *AdipoR1* or *AdipoR2* mRNA levels and any of the clinicopathological characteristics (Table 1).

4. Discussion

We have previously shown that the low serum adiponectin levels are associated with a high breast cancer risk [18], suggesting that adiponectin might be involved in the pathogenesis of breast cancer. Since very recently the receptors for adiponectin (AdipoR1 and AdipoR2) have been identified, we have investigated, in the present study, whether or not the normal breast epithelial cells and the breast cancer cells express *AdipoR1* and *AdipoR2* mRNA in order to demonstrate a possible, direct involvement of adiponectin in the breast carcinogenesis. We have been able to show that both *AdipoR1* and *AdipoR2* mRNA, but *adiponectin* mRNA, are expressed in the LMD normal breast epithelial cells and the normal breast epithelial cell lines, suggesting that the serum adiponectin produced from the adipose tissue might affect the growth of the breast epithelial cells in an endocrine, but not an autocrine, manner. Furthermore, we have confirmed the protein expression of AdipoR1 and AdipoR2 both in normal breast epithelial cells and breast cancer cells by immunostaining.

Adiponectin has been shown to directly inhibit the growth of vascular smooth muscle and endothelial cell proliferation [13] as well as myelomonocytic progenitor cells [12]. Thus, it is speculated that the serum adiponectin inhibits the growth of the normal breast epithelial cells, and a down-regulation of the serum adiponectin levels might result in the growth stimulation of the normal breast epithelial cells, leading to the high susceptibility to breast
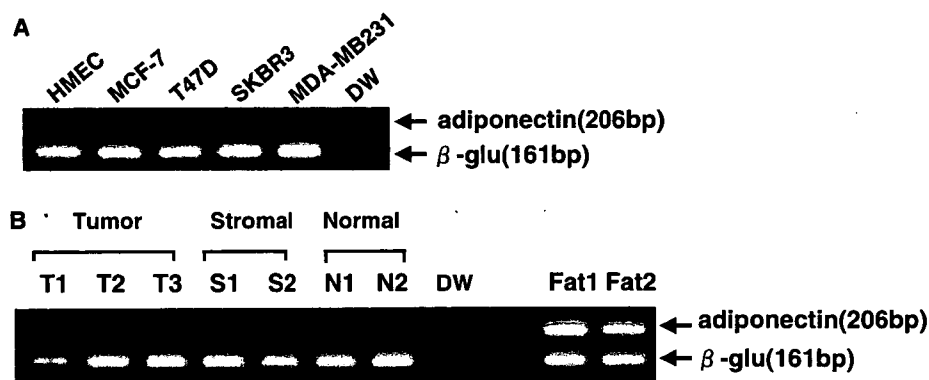

Fig. 1. *Adiponectin* mRNA expression in various cell lines and tissues determined by RT-PCR assay. (A) Lanes HMEC, MCF-7, T47D, SKBR3, MDA-MB231, and DW (negative control, distilled water). (B) Lanes T1–T3 (breast cancer cells collected by LMD from three breast tumors), lanes S1 and S2 (stromal cells collected by LMD from two breast tissues), lanes N1 and N2 (normal breast epithelial cells collected by LMD from two normal breast tissues), lane DW (negative control, distilled water), and lanes Fat1 and Fat2 (axillary adipose tissues). β-glu, β-glucuronidase.

AdipoR1

← β-glu (161bp)
← AdipoR1(101bp)

AdipoR2
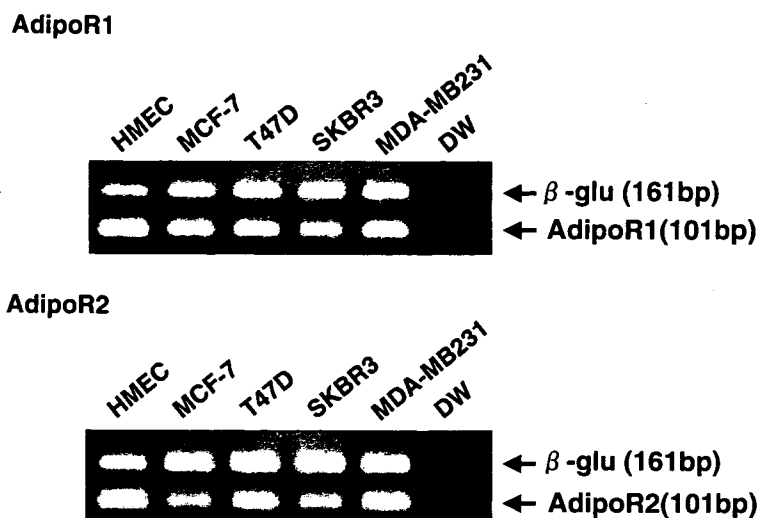
← β-glu (161bp)
← AdipoR2(101bp)

Fig. 2. *AdipoR1* and *AdipoR2* mRNA expression in various cell lines determined by RT-PCR assay. Upper panel (*AdipoR1* mRNA) and lower panel (*AdipoR2* mRNA). β-glu, β-glucuronidase.

AdipoR1

Tumor   Stromal   Normal

T1 T2 T3 T4 T5 T6   S1 S2 S3   N1 N2 DW

← β-glu(161bp)
← AdipoR1(101bp)

AdipoR2

Tumor   Stromal   Normal

T1 T2 T3 T4 T5 T6   S1 S2 S3   N1 N2 DW
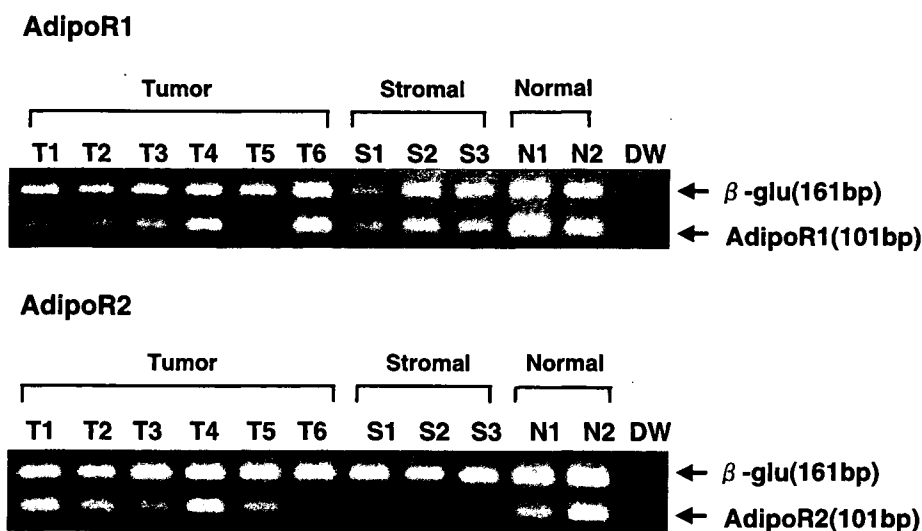
← β-glu(161bp)
← AdipoR2(101bp)

Fig. 3. *AdipoR1* and *AdipoR2* mRNA expression determined by RT-PCR assay in breast cancer cells, stromal cells, and normal breast epithelial cells collected by LMD. Upper panel (*AdipoR1* mRNA) and lower panel (*AdipoR2* mRNA): lanes T1–T6 (breast cancer cells collected by LMD from six breast tumors), lanes S1–S3 (stromal cells collected by LMD from three breast tissues), lanes N1 and N2 (normal breast epithelial cells collected by LMD from two normal breast tissues), and lane DW (negative control, distilled water). β-glu, β-glucuronidase.

carcinogenesis. This speculation is supported by the in vitro studies which demonstrate the growth inhibition of breast cancer cells by adiponectin [26,27]. Since there was no significant difference in the mRNA expression level of both *AdipoR1* and *AdipoR2* mRNA between normal breast epithelial cells and breast cancer cells (data not shown), low adiponectin level seems to play a more important role in

breast carcinogenesis than down-regulation of adiponectin receptors.

In addition, Brakenhielm et al. has recently demonstrated that adiponectin is an inhibitor of angiogenesis in vivo [28]. Since tumor growth is tightly linked to angiogenesis, angiogenesis induced by low adiponectin levels might play some role in breast carcinogenesis. We have found that
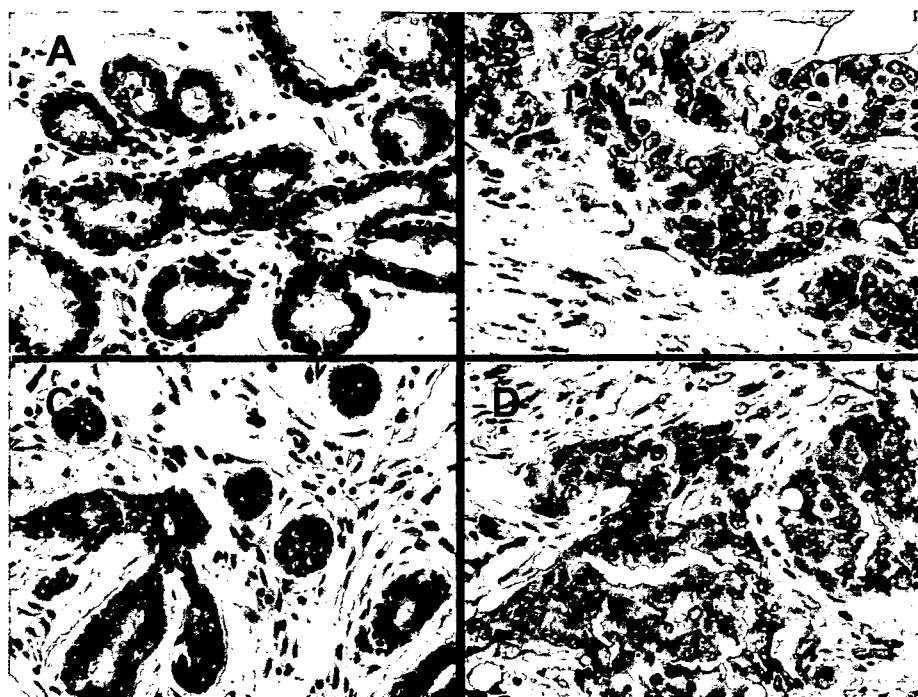
C. Takahata et al. / Cancer Letters 250 (2007) 229–236

Fig. 4. Imunohistochemical staining of AdipoR1 and AdipoR2 in normal breast tissues and breast cancer tissues (400×). AdipoR1 expression was observed in normal breast epithelial cells (A) and breast cancer cells and stromal cells (B), and AdipoR2 expression was observed in normal breast epithelial cells (C) and breast cancer cells but not stromal cells (D).

Table 1
AdipoR1 and *AdipoR2* mRNA expression and clinicopathological characteristics of breast cancers

	Number	*AdipoR1* mRNA[a]	*AdipoR2* mRNA [a]
Menopausal status			
Premenopausals	40	525.6 ± 83.9	2.38 ± 0.31
Postmenopausals	60	613.5 ± 72.0	3.65 ± 0.52
Tumor size			
⩽2 cm	48	555.1 ± 79.3	3.46 ± 0.61
>2 cm	52	599.7 ± 75.9	2.84 ± 0.35
Lymph node metastasis			
Negative	70	541.2 ± 62.0	3.23 ± 0.41
Positive	30	664.9 ± 110.5	2.92 ± 0.64
Histological grade			
1	28	575.1 ± 120.0	3.16 ± 0.75
2	46	586.7 ± 81.8	3.26 ± 0.54
3	26	566.9 ± 85.6	2.90 ± 0.46
Estrogen receptor			
Positive	70	615.7 ± 72.6	3.50 ± 0.46
Negative	30	500.0 ± 65.3	2.30 ± 0.31

[a] mRNA levels of *AdipoR1* and *AdipoR2* were shown as mean ± SE.

AdipoR1, but not AdipoR2, is expressed in stromal cells, suggesting that adiponectin affects not only the breast epithelial cells or breast cancer cells but also stromal cells through AdipoR1. Biological significance of AdipoR1 expression in stromal cells and its implication in carcinogenesis seem to deserve a further study.

In the previous study, we have shown that breast tumors developing in patients with the low adiponectin levels are associated with biologically more aggressive phenotypes such as large tumor size, high lymph node positivity, and high histological grade than those developing in patients with the high adiponectin levels [18]. Thus, it was speculated that the expression levels of *AdipoR1* and *AdipoR2* mRNA in breast tumors might affect the biological phenotypes since the expression levels of these receptors were considered to influence the responsiveness to the serum adiponectin. Thus, we have studied the relationship between *AdipoR1* or *AdipoR2* mRNA levels and the various clinicopathological characteristics of breast tumors but we have failed to show any significant association between them. Therefore, the clinical significance of *AdipoR1* and *AdipoR2* mRNA levels in breast tumors is currently unknown.

In conclusion, we have shown that *AdipoR1* and *AdipoR2* mRNA, but not *adiponectin* mRNA, are

expressed in the normal breast epithelial cells and breast cancer cells. These results seem to suggest a possibility that the association of low serum adiponectin levels with a high breast cancer risk might be explained, at least in part, by the direct effect of adiponectin on the breast epithelial cells.

Acknowledgements

References

[1] L.M. Morimoto, E. White, Z. Chen, R.T. Chlebowski, J. Hays, L. Kuller, et al., Obesity, body size, and risk of postmenopausal breast cancer: the Women's Health Initiative (United States), Cancer Causes Control 13 (2002) 741–751.

[2] K. Hirose, K. Tajima, N. Hamajima, T. Takezaki, M. Inoue, T. Kuroishi, et al., Association of family history and other risk factors with breast cancer risk among Japanese premenopausal and postmenopausal women, Cancer Causes Control 12 (2001) 349–358.

[3] C.E. Bird, S. Cook, S. Owen, E.E. Sterns, A.F. Clark, Plasma concentrations of C-19 steroids, estrogens, FSH, LH and prolactin in post-menopausal women with and without breast cancer, Oncology 38 (1981) 365–368.

[4] J.W. Moore, G.M. Clark, R.D. Bulbrook, J.L. Hayward, J.T. Murai, G.L. Hammond, et al., Serum concentrations of total and non-protein-bound oestradiol in patients with breast cancer and in normal controls, Int. J. Cancer 29 (1982) 17–21.

[5] L. Bernstein, R.K. Ross, M.C. Pike, J.B. Brown, B.E. Henderson, Hormone levels in older women: a study of postmenopausal breast cancer patients and healthy population controls, Br. J. Cancer 61 (1990) 298–302.

[6] P.G. Toniolo, M. Levitz, A. Zeleniuch-Jacquotte, S. Banerjee, K.L. Koenig, R.E. Shore, et al., A prospective study of endogenous estrogens and breast cancer in postmenopausal women, J. Natl. Cancer Inst. 87 (1995) 190–197.

[7] H.V. Thomas, T.J. Key, D.S. Allen, J.W. Moore, M. Dowsett, I.S. Fentiman, et al., A prospective study of endogenous serum hormone concentrations and breast cancer risk in post-menopausal women on the island of Guernsey, Br. J. Cancer 76 (1997) 401–405.

[8] P.K. Verkasalo, H.V. Thomas, P.N. Appleby, G.K. Davey, T.J. Key, Circulating levels of sex hormones and their relation to risk factors for breast cancer: a cross-sectional study in 1092 pre- and postmenopausal women (United Kingdom), Cancer Causes Control 12 (2001) 47–59.

[9] S.E. Hankinson, W.C. Willett, J.E. Manson, G.A. Colditz, D.J. Hunter, D. Spiegelman, et al., Plasma sex steroid hormone levels and risk of breast cancer in postmenopausal women, J. Natl. Cancer Inst. 90 (1998) 1292–1299.

[10] K. Maeda, K. Okubo, I. Shimomura, T. Funahashi, Y. Matsuzawa, K. Matsubara, cDNA cloning and expression of a novel adipose specific collagen-like factor, apM1 (AdiPose Most abundant Gene transcript 1), Biochem. Biophys. Res. Commun. 221 (1996) 286–289.

[11] Y. Nakano, T. Tobe, N.H. Choi-Miura, T. Mazda, M. Tomita, Isolation and characterization of GBP28, a novel gelatin-binding protein purified from human plasma, J. Biochem. (Tokyo) 120 (1996) 803–812.

[12] T. Yokota, K. Oritani, I. Takahashi, J. Ishikawa, A. Matsuyama, N. Ouchi, et al., Adiponectin, a new member of the family of soluble defense collagens, negatively regulates the growth of myelomonocytic progenitors and the functions of macrophages, Blood 96 (2000) 1723–1732.

[13] Y. Arita, S. Kihara, N. Ouchi, K. Maeda, H. Kuriyama, Y. Okamoto, et al., Adipocyte-derived plasma protein, adiponectin, acts as a platelets growth factor-BB-binding protein and regulates growth factor-induced common postreceptor signal in vascular smooth muscle cell, Circulation 105 (2002) 2893–2898.

[14] T. Yamauchi, J. Kamon, H. Waki, Y. Terauchi, N. Kubota, K. Hara, et al., The fat-derived hormone adiponectin reverses insulin resistance associated with both lipoatrophy and obesity, Nat. Med. 7 (2001) 941–946.

[15] J. Fruebis, T.S. Tsao, S. Javorschi, D. Ebbets-Reed, M.R. Erickson, F.T. Yen, et al., Proteolytic cleavage product of 30-kDa adipocyte complement-related protein increases fatty acid oxidation in muscle and causes weight loss in mice, Proc. Natl. Acad. Sci. USA 98 (2001) 2005–2010.

[16] A.H. Berg, T.P. Combs, X. Du, M. Brownlee, P.E. Scherer, The adipocyte-secreted protein Acrp30 enhances hepatic insulin action, Nat. Med. 7 (2001) 947–953.

[17] N. Maeda, I. Shimomura, K. Kishida, H. Nishizawa, M. Matsuda, H. Nagaretani, et al., Diet-induced insulin resistance in mice lacking adiponectin/ACRP30, Nat. Med. 8 (2002) 731–737.

[18] Y. Miyoshi, T. Funahashi, S. Kihara, T. Taguchi, Y. Tamaki, Y. Matsuzawa, et al., Association of serum adiponectin levels with breast cancer risk, Clin. Cancer Res. 9 (2003) 5699–5704.

[19] C. Mantzoros, E. Petridou, N. Dessypris, C. Chavelas, M. Dalamaga, D.M. Alexe, et al., Adiponectin and breast cancer risk, J. Clin. Endocrinol. Metab. 89 (2004) 1102–1107.

[20] L. Dal Maso, L.S. Augustin, A. Karalis, R. Talamini, S. Franceschi, D. Trichopoulos, et al., Circulating adiponectin and endometrial cancer risk, J. Clin. Endocrinol. Metab. 89 (2004) 1160–1163.

[21] A. Bergstrom, P. Pisani, V. Tenet, A. Wolk, H.O. Adami, Overweight as an avoidable cause of cancer in Europe, Int. J. Cancer 91 (2001) 421–430.

[22] T. Yamauchi, J. Kamon, Y. Ito, A. Tsuchida, T. Yokomizo, S. Kita, et al., Cloning of adiponectin receptors that mediate antidiabetic metabolic effects, Nature 423 (2003) 762–769.

[23] I. Kharroubi, J. Rasschaert, D.L. Eizirik, M. Cnop, Expression of adiponectin receptors in pancreatic beta cells, Biochem. Biophys. Res. Commun. 312 (2003) 1118–1122.

[24] G. Chinetti, C. Zawadski, J.C. Fruchart, B. Staels, Expression of adiponectin receptors in human macrophages and regulation by agonists of the nuclear receptors PPARalpha,

PPARgamma, and LXR, Biochem. Biophys. Res. Commun. 314 (2004) 151–158.

[25] H.S. Berner, S.P. Lyngstadaas, A. Spahr, M. Monjo, L. Thommesen, C.A. Drevon, et al., Adiponectin and its receptors are expressed in bone-forming cells, Bone 35 (2004) 829–842.

[26] J.H. Kang, Y.Y. Lee, B.Y. Yu, B.S. Yang, K.H. Cho, D.K. Yoon, et al., Adiponectin induces growth arrest and apoptosis of MDA-MB-231 breast cancer cell, Arch. Pharm. Res. 28 (2005) 1263–1269.

[27] M.N. Dieudonne, M. Bussiere, E.D. Santos, M.C. Leneveu, Y. Giudicelli, R. Pecquery, Adiponectin mediates antiproliferative and apoptotic responses in human MCF7 breast cancer cells, Biochem. Biophys. Res. Commun. 345 (2006) 271–279.

[28] E. Brakenhielm, N. Veitonmaki, R. Cao, S. Kihara, Y. Matsuzawa, B. Zhivotovsky, et al., Adiponectin-induced antiangiogenesis and antitumor activity involve caspase-mediated endothelial cell apoptosis, Proc. Natl. Acad. Sci. USA 101 (2004) 2476–2481.

Imaging, Diagnosis, Prognosis

One-step Nucleic Acid Amplification for Intraoperative Detection of Lymph Node Metastasis in Breast Cancer Patients

Masahiko Tsujimoto,[1] Kadzuki Nakabayashi,[14] Katsuhide Yoshidome,[2] Tomoyo Kaneko,[8] Takuji Iwase,[9] Futoshi Akiyama,[8] Yo Kato,[8] Hitoshi Tsuda,[12] Shigeto Ueda,[13] Kazuhiko Sato,[13] Yasuhiro Tamaki,[3] Shinzaburo Noguchi,[3] Tatsuki R. Kataoka,[4] Hiromu Nakajima,[5] Yoshifumi Komoike,[6] Hideo Inaji,[6] Koichiro Tsugawa,[11] Koyu Suzuki,[10] Seigo Nakamura,[11] Motonari Daitoh,[14] Yasuhiro Otomo,[14] and Nariaki Matsuura[7]

Abstract

Purpose: Detection of sentinel lymph node (SLN) metastasis in breast cancer patients has conventionally been determined by intraoperative histopathologic examination of frozen sections followed by definitive postoperative examination of permanent sections. The purpose of this study is to develop a more efficient method for intraoperative detection of lymph node metastasis.

Experimental Design: Cutoff values to distinguish macrometastasis, micrometastasis, and nonmetastasis were determined by measuring cytokeratin 19 (CK19) mRNA in histopathologically positive and negative lymph nodes using one-step nucleic acid amplification (OSNA). In an intraoperative clinical study involving six facilities, 325 lymph nodes (101 patients), including 81 SLNs, were divided into four blocks. Alternate blocks were used for the OSNA assay with CK19 mRNA, and the remaining blocks were used for H&E and CK19 immunohistochemistry–based three-level histopathologic examination. The results from the two methods were then compared.

Results: We established CK19 mRNA cutoff values of 2.5×10^2 and 5×10^3 copies/μL. In the clinical study, an overall concordance rate between the OSNA assay and the three-level histopathology was 98.2%. Similar results were obtained with 81 SLNs. The OSNA assay discriminated macrometastasis from micrometastasis. No false positive was observed in the OSNA assay of 144 histopathologically negative lymph nodes from pN0 patients, indicating an extremely low false positive for the OSNA assay.

Conclusion: The OSNA assay of half of a lymph node provided results similar to those of three-level histopathology. Clinical results indicate that the OSNA assay provides a useful intraoperative detection method of lymph node metastasis in breast cancer patients.

Authors' Affiliations: Departments of [1]Pathology and [2]Surgery, Osaka Police Hospital, [3]Department of Breast and Endocrine Surgery, Osaka University Graduate School of Medicine, Departments of [4]Pathology, [5]Clinical Laboratory, and [6]Surgery, Osaka Medical Center for Cancer and Cardiovascular Diseases, and [7]Department of Molecular Pathology, Osaka University Graduate School of Medicine and Health Science, Osaka, Japan; Departments of [8]Pathology and [9]Breast Surgery, Cancer Institute of the Japanese Foundation for Cancer Research, and Departments of [10]Pathology and [11]Breast Surgical Oncology, St. Luke's International Hospital, Tokyo, Japan; Departments of [12]Pathology II and [13]Surgery I, National Defense Medical College, Saitama, Japan; and [14]Central Research Laboratories, Sysmex Corp., Kobe, Japan

Sentinel lymph node (SLN) biopsy has recently become a standard surgical procedure in the treatment of breast cancer patients (1–10). This procedure can predict metastasis to the regional lymph nodes with high accuracy and avoids unnecessary removal of axillary lymph nodes and subsequent morbidity associated with axially clearance in node negative breast cancer patients.

SLN metastasis is generally detected by conventional means including the intraoperative H&E-based histopathologic examination of frozen section(s) or cytologic observation of touch-imprints, followed by definitive postoperative histopathologic examination of permanent sections (2, 7–9). However, the sensitivity of these intraoperative methods is not high. Many investigators have reported that the intraoperative H&E-based histopathologic examination has a false-negative rate of 5% to 52% (reviewed in ref. 11). Furthermore, these methods provide subjective rather than objective results, which may differ from one pathologist to another (12). On the other hand, the definitive postoperative histopathologic examination generally requires 5 to 10 days for assessment. If an accurate

intraoperative method is developed, the test results can allow for completion of axillary node dissection during surgery and avoidance of a second surgical procedure in patients with positive SLNs, thereby reducing patient distress and, finally, saving hospital costs (2, 13, 14). Accordingly, the development of a precise and objective intraoperative method for the detection of lymph node metastasis is important for increasing the efficiency of breast cancer surgery (10, 13 - 18).

To overcome the shortcomings of the present histopathologic methods, molecular biological methods based on quantitative reverse transcription-PCR (QRT-PCR) have been studied extensively for the detection of lymph node metastasis in breast cancer patients (12, 19-25). A QRT-PCR assay with multiple mRNA markers including cytokeratin 19 (CK19), trefoil factor 3 (p1B), epithelial glycoprotein 2 (EGP2), and small breast epithelial mucin (SBEM) resulted in a 10% upstaging compared with the routine histopathologic analysis (22). It was also reported that a QRT-PCR assay using mRNA markers of CK19 and mammaglobin 1 (MGB1) was almost as accurate (94.1% sensitivity and 98.6% specificity) as that of the conventional histopathologic examination (12). This study included a discussion of the drawbacks of using a single marker like CK19 mRNA for which the QRT-PCR may include the concomitant amplification of CK19 pseudogenes within genomic DNA, giving false positive results.

We recently developed a one-step nucleic acid amplification (OSNA) assay (Fig. 1A), which consists of solubilization of a lymph node followed by reverse-transcription loop-mediated isothermal amplification (RT-LAMP) of a target mRNA (26, 27). The RT-LAMP reaction is a new method of gene amplification, and its application has been reported previously (28-32). The OSNA method is characterized by the quantitative measurement of a target mRNA in a metastatic lymph node, a brief reaction time for the OSNA process, a high specificity for the target mRNA, and an absence of genomic DNA amplification.

In this paper, we report an efficient intraoperative detection method for lymph node metastasis in breast cancer patients using the OSNA assay with CK19 mRNA as a target marker. The results of a multicenter clinical study including 325 lymph nodes are discussed from the viewpoint of the usefulness of the OSNA assay as an intraoperative detection method.

Materials and Methods

Lymph nodes for selection of mRNA markers and determination of cutoff values. Lymph nodes, which were used to select mRNA markers and determine cutoff values, were obtained from Osaka Police Hospital with the approval of its internal review board. Lymph nodes were stored at -80°C until use.

QRT-PCR. QRT-PCR was carried out by ABI Prism 7700 sequence detector. RNA was purified from a lymph node lysate using RNeasy Mini Kit (Qiagen), and then purified RNA was subjected to one-step RT-PCR with QuantiTect SYBR Green (Qiagen) according to the manufacturer's instructions. The sequences of the forward and reverse primers used are shown in Supplementary Table S1. The primers were designed by Primer Express Version 2.0 software (ABI).

Selection of mRNA maker. Forty-five candidate mRNA markers, selected as being specific to breast cancer tissue, were identified from the public EST database (33). The performance of these mRNA markers was evaluated with QRT-PCR using a mixture of four histopathologically positive and four negative lymph nodes. The results were summarized as C_t (threshold cycle) values for each mRNA marker (see Supplementary Table S2). The selected markers, KRT19 (CK19), CEACAM5 (CEA), forkhead box A1 (FOXA1), SAM-pointed domain containing ETS transcription factor (SPDEF), tumor-associated calcium signal transducer 2 (TACSTD-2), mucin 1 (MUC1), and MGB1, were further evaluated with QRT-PCR using 11 histopathologically positive and 15 negative lymph nodes from 26 patients.

RT-LAMP reaction of CK19 mRNA. The RT-LAMP reaction was carried out according to the Notomi's method (26, 27). The human CK19 mRNA was synthesized by *in vitro* transcription from cloned cDNA.

A 2-μL sample of human CK19 mRNA in a lysis buffer containing 200 mmol/L glycine-HCl, 20% DMSO, and 5% Brij35 (pH 3.5) was added to 23 μL of solution consisting of 3.5 μmol/L each of the forward inner (CK19FA) and reverse primer (CK19RA), 0.2 μmol/L each of forward outer (CK19F3) and reverse primer (CK19R3), 2.6 μmol/L each of forward loop (CK19LPF) and reverse primer (CK19LPR), 0.9 mmol/L deoxynucleotide triphosphates, 54.3 mmol/L Tris-HCl, 10.8 mmol/L KCl, 10.8 mmol/L $(NH_4)_2SO_4$, 5.4 mmol/L $MgSO_4$, 0.1% Triton X-100, 5.4 mmol/L DTT, 2.5 units avian myeloblastosis virus reverse transcriptase (Promega), 18 units Bst DNA Polymerase (New England Biolabs), and 25 units RNasin Plus (Promega). Each reaction mixture contained three pairs of primer sets including the loop primer (27). The sequences of the human CK19 primers were designed as amplicons spanning exon junction regions between CK19 exons 1 and 2 and were
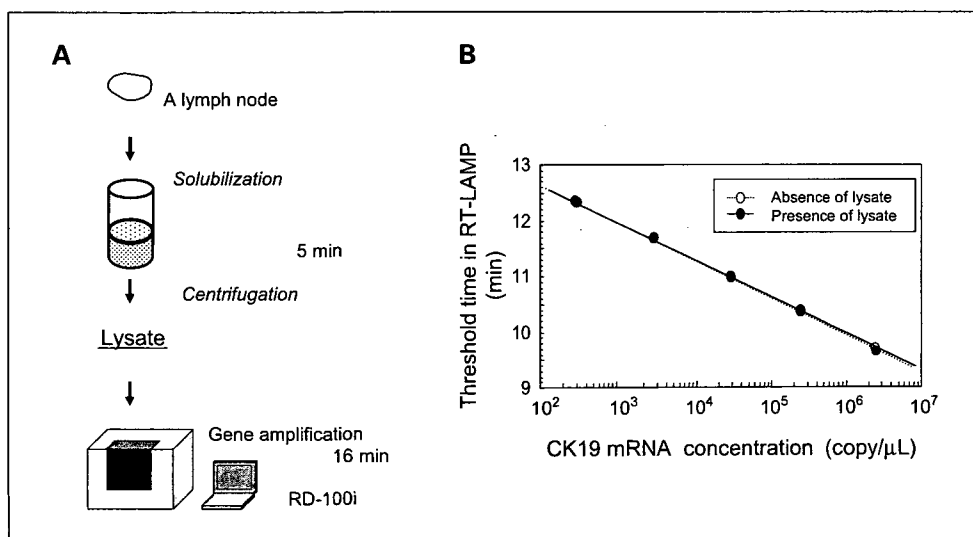

Fig. 1. OSNA assay. *A,* schematic diagram of the OSNA procedure. *B,* standard curve of human CK19 mRNA measured by RD-100i in the presence and absence of lymph node lysate. A histopathologically negative lymph node (600 mg) was homogenized in 4 mL of lysis buffer. A 180-μL sample of the lymph node lysate was added to 20 μL of human CK19 mRNA in the lysis buffer. The final concentration of human CK19 mRNA was adjusted to 2.5×10^6, 2.5×10^5, 2.5×10^4, 2.5×10^3, and 2.5×10^2 copies/μL. A 2-μL sample of each was subjected to the RT-LAMP reaction under the same conditions described in Materials and Methods.

Fig. 2. A schematic representation of primer placement along the CK19 cDNA sequence. The CK19 cDNA sequence (NM.002276) and the sequence of the primers for the CK19 RT-LAMP are shown. The location on CK19 cDNA where each primer-set binds is underlined. The sequence of the inner primer (FA and RA) consists of discontinuous two different regions, F1c and F2 (or R1c and R2), to create the stem structure during the RT-LAMP reaction. The exon junction between exons 2 and 3 is included in the sequence of the R2 region in the RA primer (arrowhead).

```
                                    F3 primer
461 AGGTGAAGAT CCGCGACTGG TACCAGAAGC AGGGGCCTGG GCCCTCCCGC
    TCCACTTCTA GGCGCTGACC ATGGTCTTCG TCCCCGGACC CGGGAGGGCG


                        FA primer (F2)
511 GACTACAGCC ACTACTACAC GACCATCCAG GACCTGCGGG ACAAGATTCT
    CTGATGTCGG TGATGATGTG CTGGTAGGTC CTGGACGCCC TGTTCTAAGA
                                                LPF primer
                                RA primer (R1c)
561 TGGTGCCACC ATTGAGAACT CCAGGATTGT CCTGCAGATC GACAATGCCC
    ACCACGGTGG TAACTCTTGA GGTCCTAACA GGACGTCTAG CTGTTACGGG
            FA primer (F1c)

        LPR primer                      ▼
611 GTCTGGCTGC AGATGACTTC CGAACCAAGT TTGAGACGGA ACAGGCTCTG
    CAGACCGACG TCTACTGAAG GCTTGGTTCA AACTCTGCCT TGTCCGAGAC
                                RA primer (R2)


661 CGCATGAGCG TGGAGGCCGA CATCAACGGC CTGCGCAGGG
    GCGTACTCGC ACCTCCGGCT GTAGTTGCCG GACGCGTCCC
                        R3 primer
```

furthermore designed as mismatch sequences of the CK19a and CK19b pseudogenes (GenBank accession number M33101 and U85961) using Probe Wizard (RNAture). Primer sequences were 5′-GGAGTTCT-CAATGGTGGCACCAACTACTACACGACCATCCA-3′ (CK19FA), 5′-GTCCTGCAGATCGACAACGCCTCCGTCTCAAACTTGGTTCG-3′ (CK19RA), 5′-TGGTACCAGAAGCAGGGG-3′ (CK19F3), 5′-GTTGATGTCGGCCTCCACG-3′ (CK19R3), 5′-AGAATCTTGTCCCG-CAGG-3′ (CK19LPF), and 5′-CGTCTGGCTGCAGATGA-3′ (CK19LPR). The sequence of each primer and its placement along the CK19 cDNA sequence are shown in Fig. 2.

The RT-LAMP reaction with CK19 mRNA was carried out in a gene amplification detector, RD-100i (Sysmex). Mori et al. (34, 35) reported that PPi, which is produced in the course of the RT-LAMP reaction, binds to magnesium ion to result in magnesium PPi. The amount of magnesium PPi increases with the passage of the reaction. Magnesium PPi has a low solubility in aqueous solution and precipitates when its concentration reaches saturation. The amplification of CK19 mRNA was monitored by measuring the turbidity of the reaction mixture at 6-s intervals. The threshold time was defined as the time at which the turbidity exceeded 0.1.

OSNA assay. A schematic diagram of the OSNA assay with CK19 mRNA is shown in Fig. 1A. A histopathologically negative lymph node (≤600 mg) was homogenized in 4 mL of the above lysis buffer for 90 s on ice using a Physicotron Warring blender with an NS-4 shaft (MicroTec Nichion). The homogenate was centrifuged at 10,000 × g for 1 min at room temperature. A 2-μL sample of the supernatant (lysate) was subjected to the RT-LAMP reaction under the same conditions as above. CK19 mRNA copy number was determined based on the standard curve using a known quantity of human CK19 mRNA.

Effect of lymph node size on the OSNA assay. A histopathologically negative lymph node (130 mg) was homogenized in 4 mL of lysis buffer under the same conditions as above. A 180-μL sample of lymph node lysate was added to 20 μL of human CK19 mRNA in the lysis buffer. The final concentration of human CK19 mRNA was adjusted to 2.5 × 10^5 and 2.5 × 10^3 copies/μL. About 2 μL of each sample was subjected to the RT-LAMP reaction under the same conditions described above. Each sample was assayed in duplicate. Other histopathologically negative lymph nodes (214, 354, and 428 mg) were treated under the same conditions as above.

Amplification of genomic DNA by the OSNA assay. Genomic DNA was extracted from histopathologically positive lymph nodes using QIAamp DNA Mini Kit (Qiagen) according to the manufacturer's instructions. Purified genomic DNA (100 ng) was subjected to the OSNA assay using the CK19 primers described above.

Protocol for determining the cutoff values. A cutoff value (L) for the OSNA assay between metastatic positive and negative lymph nodes was determined using 106 lymph nodes (42 histopathologically negative lymph nodes from pN0 patients, 42 histopathologically negative lymph nodes from pN1-3 patients, and 22 histopathologically positive lymph nodes) from 30 patients (24 ductal carcinomas, 5 special types, and 1 ductal carcinoma in situ). As shown in Fig. 3A, the central part of one quarter of a frozen lymph node (40-600 mg) of 1 mm thickness was dissected out. Four levels (i, ii, iii, and iv) were used as permanent slices for the histopathologic examination with H&E and immunohisto-chemistry using anti-CK19 antibody (DAKO) as shown in Fig. 3A.

Histopathologically positive lymph nodes were defined as those that were positive at any of four levels (i, ii, iii, and iv). Histopathologically negative lymph nodes were defined as those that were negative in all four levels. Blocks a and c were used for the OSNA assay. A cutoff value was determined by statistical analysis of the copy numbers obtained by the OSNA assay of the histopathologically negative lymph nodes from pN0 patients.

According to the tumor-node-metastasis (TNM) classification of the Unio Internationale Contra Cancrum (Italian) sixth and the American Joint Committee on Cancer sixth editions (36), macrometastasis is defined as having metastatic foci of ≥2 mm in the long axis. In the OSNA assay, macrometastasis is assumed as having the amount of CK19 mRNA expression in 2^3 mm^3 of metastatic foci. Based on this assumption, we estimated a cutoff value (H) for CK19 mRNA between macrometastasis and micrometastasis as follows. Nine frozen histopathologically positive lymph nodes from nine breast cancer patients (8 ductal and 1 lobular carcinomas) were used to estimate the amount of CK19 mRNA expression in 2^3 mm^3 of metastatic foci (Table 1). A frozen lymph node was serially sectioned at 10-μm intervals. Each slice was first examined with CK19 immunohistochemistry-based histopathologic examination to measure the area of metastatic foci and then with RT-LAMP to measure CK19 mRNA expression. The procedure is detailed in Fig. 3B.
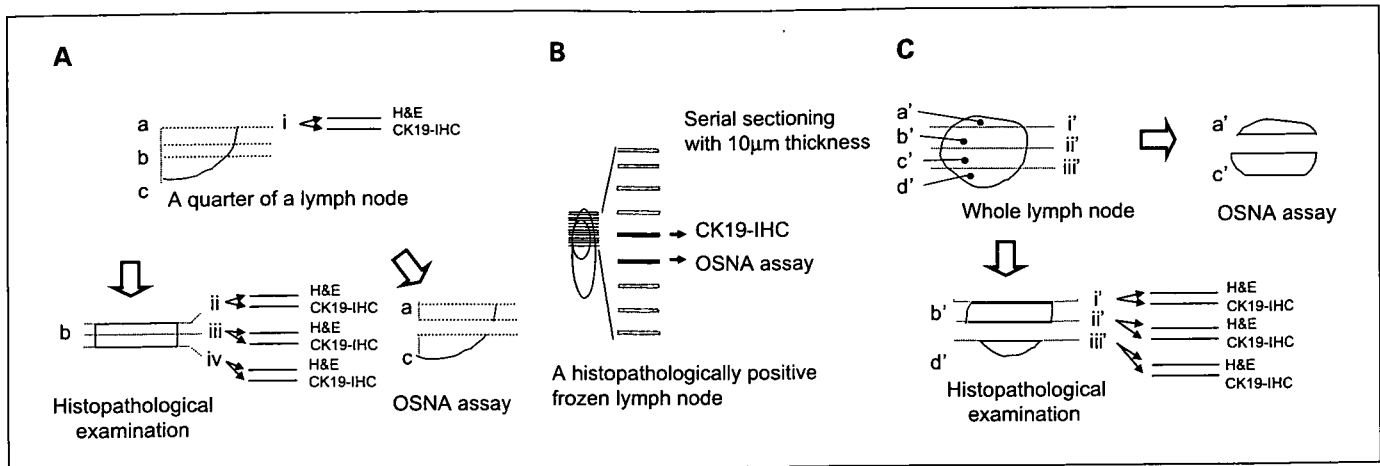
Fig. 3. Protocols. *A,* protocol for determining a cutoff value for micrometastasis and nonmetastasis. *B,* protocol for determining the cutoff value between macrometastasis and micrometastasis. Serial frozen sections taken at 10-μm intervals were prepared from histopathologically positive lymph nodes. One of two consecutive frozen sections was subjected to CK19 immunohistochemistry (CK19-IHC) – based histopathologic examination to measure the area of metastatic foci, and then the volume of the metastatic foci was calculated by multiplying the area by the thickness of the slice. The adjacent section was subjected to the OSNA assay. The expression level of CK19 mRNA in 2^3 mm^3 was estimated based on the correlation between the volume of metastatic foci and CK19 mRNA expression. *C,* clinical study protocol.

In the OSNA assay, an amount of CK19 mRNA expression less than the cutoff value was indicated as (-), an amount of CK19 mRNA expression between the cutoff values L and H was indicated as (+), and an amount of CK19 mRNA expression greater than the cutoff value H was indicated as (++).

Clinical study protocol. An intraoperative clinical study was conducted from February 2005 to July 2005 at six facilities other than Sysmex Central Research Laboratories. A total of 325 fresh lymph nodes (101 patients), including 81 SLNs (49 patients), were used with the approval of the internal review board at each facility. The clinicopathologic characteristics of patients are shown in Table 2. A large percent of patients had stages I A/B and II A/B. The majority of patients had a nodal status of pN0 and pN1. About 80% of patients had invasive ductal carcinoma.

A fresh lymph node with a short axis of 4 to 12 mm was divided into four blocks at 1- or 2-mm intervals using our original cutting device (Fig. 3C and 4). Blocks a′ and c′ were used for the OSNA assay. Two slices were cut from each of the three cutting surfaces (i′, ii′, and iii′), as shown in Fig. 3C, and used for the permanent three-level histopathologic examination with H&E and CK19 immunohistochemistry.

In the histopathologic examination, macrometastasis and micrometastasis were defined according to the TNM classification of the Unio Internationale Contra Cancrum sixth and American Joint Committee on Cancer sixth editions (36). All samples for histopathologic examination were examined by three third-party pathologists. Conflicting results were settled consensually. The performance of the OSNA assay was compared with the three-level histopathology.

The OSNA assay analyzed different blocks from those used in the three-level histopathologic examination. Therefore, in this protocol, the sensitivity and specificity of the OSNA assay could not be calculated based on the histopathologic results. For this reason, we evaluated the performance of the OSNA assay as a concordance rate with the three-level histopathologic examination.

In the case of lymph nodes from pN0 patients, blocks b′ and d′ were further sliced at 0.2-mm intervals, followed by staining each alternate slice with H&E and CK19 immunohistochemistry (Fig. 3C). A total of 144 lymph nodes, in which neither macrometastasis nor micrometastasis were observed in the above serial sectioning examination, were used for the false positive study of the OSNA assay.

When discordance between the OSNA assay and the three-level histopathologic examination occurred, a histopathologic analysis of blocks b′ and d′ was repeated. All slides for the histopathologic examination were examined and evaluated by three third-party

pathologists. All results of histopathologic examinations were finally determined by a study group comprised of representatives from the different facilities.

Analysis of discordant cases. In the analysis of discordant cases, QRT-PCR and CK19 Western blot analysis of the lysates were carried out. QRT-PCR was carried out with TaqMan RT-PCR. RNA was purified from lymph node lysates using RNeasy Mini Kit (Qiagen), and then the purified RNA was subjected to TaqMan one-step RT-PCR universal master mix (ABI) according to the manufacturer's instructions. The sequences of the forward and reverse primers designed for human CK19 were 5′-CAGATCGAAGGCCTGAAGGA-3′ and 5′-CTTGGCCCCT-CAGCCGTACT-3′, respectively. The sequence of the TaqMan probe, containing a fluorescent reporter dye (FAM) at the 5′ end and a fluorescent quencher dye (TAMRA) at the 3′ end, was 5′-FAM-GCCTACCTGAA-GAAGAACCATGAGGAGGAA-TAMRA-3′. The primers and TaqMan probe were obtained from Applied Biosystems (ABI). All QRT-PCR reactions were done in duplicate.

In the CK19 Western blot analysis, lysate (20 μL) was added to 10 μL of loading buffer containing 150 mmol/L Tris-HCl, 300 mmol/L DTT, 6% SDS, 0.3% bromophenol blue, and 30% glycerol. The solution was boiled and electrophoresed on a polyacrylamide gel in the presence of

Table 1. CK19 mRNA expression in 2^3 mm^3 of metastatic foci

Case	Histology	CK19 mRNA (copy/μL)
1	Ductal carcinoma	2.3×10^4
2	Ductal carcinoma	1.1×10^4
3	Ductal carcinoma	4.7×10^3
4	Ductal carcinoma	5.0×10^4
5	Ductal carcinoma	1.0×10^4
6	Lobular carcinoma	1.4×10^5
7	Ductal carcinoma	2.0×10^4
8	Ductal carcinoma	6.7×10^4
9	Ductal carcinoma	2.4×10^4
	Average	3.0×10^4

NOTE: CK19 mRNA expression in 2^3 mm^3 of metastatic foci was estimated on the basis of the examination of serial sections (Fig. 3B).

Table 2. Clinicopathologic characteristics of patients

	Number of patients
Stage	
0	5
I A/B	41
II A/B	49
III A/B/C	5
IV	1
Nodal status	
pN0	60
pN1	35
pN2	2
pN3	4
Histopathologic type	
Invasive ductal carcinoma	87
Neuroendocrine carcinoma	1
Matrix producing carcinoma	1
Mucinous carcinoma	2
Apocrine carcinoma	1
Invasive lobular carcinoma	4
Ductal carcinoma *in situ*	5

SDS (PAG Mini; Daiichi Pure Chemicals). After electrotransfer to Immobilon-FL polyvinylidene difluoride membranes (Millipore), the membrane was blocked with skim milk (BD Bioscience) for 1 h at room temperature. The primary antibody, anti-CK19 (A53-B/A2; Santa Cruz Biotechnology), was diluted 1:500 with TBS-Tween 20 (TBS-T) solution, and the membrane was incubated at 4°C overnight with anti-CK19 antibody. The membrane was then washed with TBS-T and incubated with a secondary antibody conjugated with horseradish peroxidase, which was diluted 1:2,000 with TBS-T. After washing the membrane twice with TBS-T, CK19-CK19 antibody complex was visualized using the ECL-Advance detection kit (GE Healthcare). The intensity of the signal in each band was evaluated by LumiAnalyst

(Roche). CK19 protein concentration was determined based on a standard curve that was obtained by measuring known quantities of CK19 protein (Biodesign) of 0.15, 0.075, 0.038, and 0.018 ng/μL.

A cutoff value for CK19 protein expression between histopathologically positive and negative lymph nodes was determined by Western blot analysis of 37 histopathologically negative lymph nodes from 16 pN0 patients, 54 histopathologically negative lymph nodes from 17 pN1-3 patients, and 22 histopathologically positive lymph nodes from 12 patients (Figs. 3A and 5A). The cutoff value was determined by statistical analysis of the amount of CK19 measured by Western blot analysis of 37 histopathologically negative lymph nodes from 16 pN0 patients.

Results

Selection of the mRNA marker. We evaluated mRNAs for CK19, CEA, FOXA1, SPDEF, MUC1, and MGB1 using 11 histopathologically positive and 15 negative lymph nodes from 26 patients. The absolute mRNA expression levels of CEA and MGB1 in metastatic lymph nodes were not as high as expected, whereas the absolute expression levels of MUC1 mRNA in nonmetastatic lymph nodes was relatively high. For these reasons, CEA, MGB1, and MUC1 mRNAs were not selected for the OSNA assay.

The expression levels of CK19, FOXA1, and SPDEF mRNAs differed between histopathologically positive and negative lymph nodes. However, the lower limits of the expression levels of FOXA1 and SPDEF mRNAs in histopathologically positive lymph nodes were 4 to 30 times less than that of CK19 mRNA (Fig. 6). On the other hand, the detection limit of the OSNA assay was nearly equivalent to 32 threshold cycles of the RT-PCR system. An assay system should detect the upper limit of the expression levels of an mRNA marker in histopathologically negative lymph nodes. The upper limits of the threshold cycle of FOXA1 and SPDEF mRNAs were about 35 and 32,

Fig. 4. Lymph node cutting device.
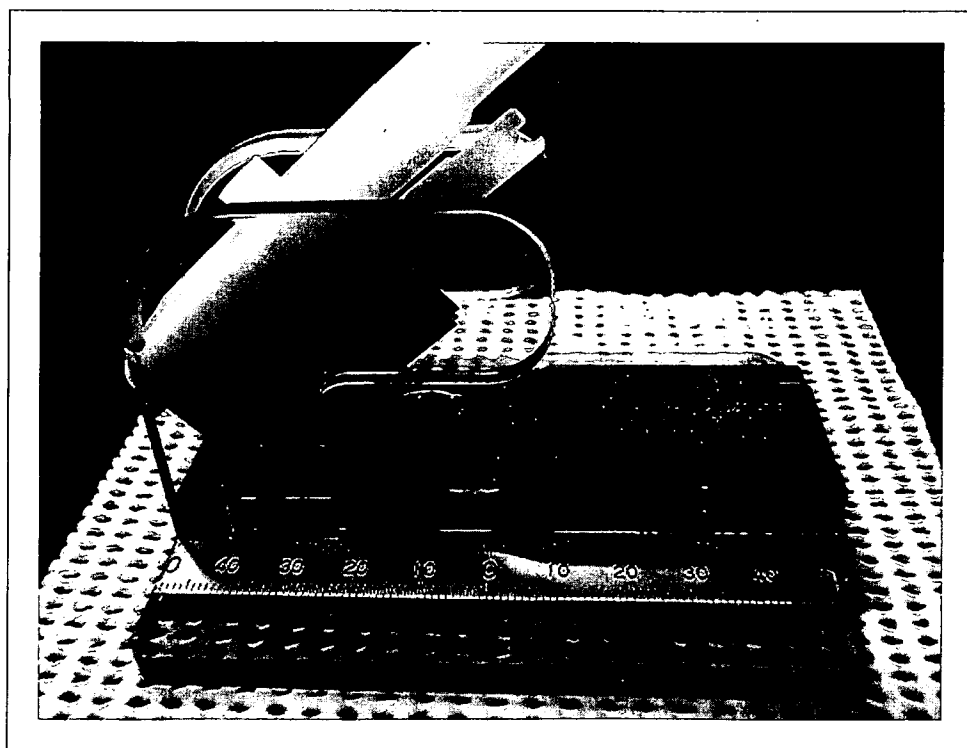
respectively. For these reasons, we determined CK19 mRNA to be the best marker for the OSNA assay.

OSNA assay. As shown in Fig. 1B, an inverse correlation between the threshold time in the RT-LAMP step and CK19 mRNA concentration was observed in a range of CK19 mRNA concentrations of 2.5×10^2 to 2.5×10^6 copies/μL, and both curves overlapped completely in the presence and absence of the lymph node lysate; the correlation coefficient value in both cases was 0.99. This result indicates that factors that may be present in lymph node lysates do not interfere with the OSNA assay.

Effect of lymph node size on the OSNA assay. The threshold time of the OSNA assay with 2.5×10^3 and 2.5×10^5 copies/μL of CK19 mRNA in a lysate obtained from 130 mg of lymph node was 10.9 and 9.6 min, respectively. The threshold time with 2.5×10^3 copies/μL of CK19 mRNA in a lysate obtained from a lymph node of 214, 354, and 428 mg was 10.7, 10.9, and 10.9 min, respectively, whereas the time with 2.5×10^5 copies/μL of CK19 mRNA in a lysate obtained from a lymph node of 214, 354, and 428 mg was 9.6, 9.7, and 9.7 min, respectively. The threshold times with 2.5×10^3 and 2.5×10^5 copies/μL of human CK19 mRNA in the lysates obtained from lymph nodes of 130, 214, 354, and 428 mg were within an acceptable error range. The results indicate that the OSNA assay is not influenced by lymph node size.

Amplification of genomic DNA by the OSNA assay. To exclude the possibility of genomic DNA amplification in the OSNA assay, we examined the OSNA assay using genomic DNA purified from lymph nodes. Genomic DNA was not amplified from either metastatic or nonmetastatic lymph nodes. The results indicate that the OSNA assay amplifies only CK19 mRNA.

Cutoff values. A cutoff value for the OSNA assay between histopathologically positive and negative lymph nodes was determined by the logarithmic normal distribution of CK19 mRNA copy numbers from 42 lymph nodes from pN0 patients. The average value of CK19 mRNA expression +3 SD was 2.5×10^2 copies/μL. Based on this analysis, we set the cutoff value at 2.5×10^2 copies/μL, which represents the upper limit of the copy numbers in the histopathologically negative lymph nodes from pN0 patients (Fig. 7A).

To validate the cutoff value, we examined CK19 mRNA expression in 42 histopathologically negative lymph nodes from 16 pN1-3 patients. Only one of these 42 cases showed >2.5×10^2 copies/μL CK19 mRNA (Fig. 7B). This lymph node showed 3×10^3 copies/μL of CK19 mRNA. This suggested that micrometastatic foci in block a or c (Fig. 3A) of the lymph node were included in the sample. On the other hand, CK19 mRNA expression in all 24 pathologically positive lymph nodes from 10 patients exceeded the cutoff value (Fig. 7C).

To obtain a cutoff value for CK19 mRNA expression between macrometastasis with metastatic foci >2^3 mm^3 and micrometastasis, we compared CK19 mRNA expression in serial sections of a lymph node with an area of metastatic foci and roughly estimated macrometastasis to be >5×10^3 copies/μL, which is the lowest value of CK19 mRNA expression found in metastatic foci of 2^3 mm^3 (Table 1).

Accordingly, for the OSNA assay, we defined macrometastasis (++) as >5×10^3 copies/μL of CK19 mRNA, micrometastasis (+) as 2.5×10^2 to 5×10^3 copies/μL, and nonmetastasis (-) as <2.5×10^2 copies/μL.

Clinical study. All OSNA assays were carried out during surgery and were completed within 30 min. H&E and CK19 immunohistochemistry were used in the histopathologic examination.

Isolated tumor cells (ITC) are widely used as one of indicators in a nomogram-aiding treatment decisions. In the American Society of Clinical Oncology guidelines (10), ITCs are described as having unknown clinical significance, and there are insufficient data to recommend appropriate treatment, including axillary lymph node dissection. For this reason, we viewed ITC as negative.

Table 3 shows the results of CK19 immunohistochemistry in all samples with the H&E results given in parenthesis. H&E-based histopathology failed to detect 1 of 40 cases of macrometastasis and 3 of 5 cases of micrometastasis. Overall, the sensitivity of H&E-based histopathology was 91.1% based on the results of CK19 immunohistochemistry–based histopathology. The sensitivities of the one- and two-level CK19
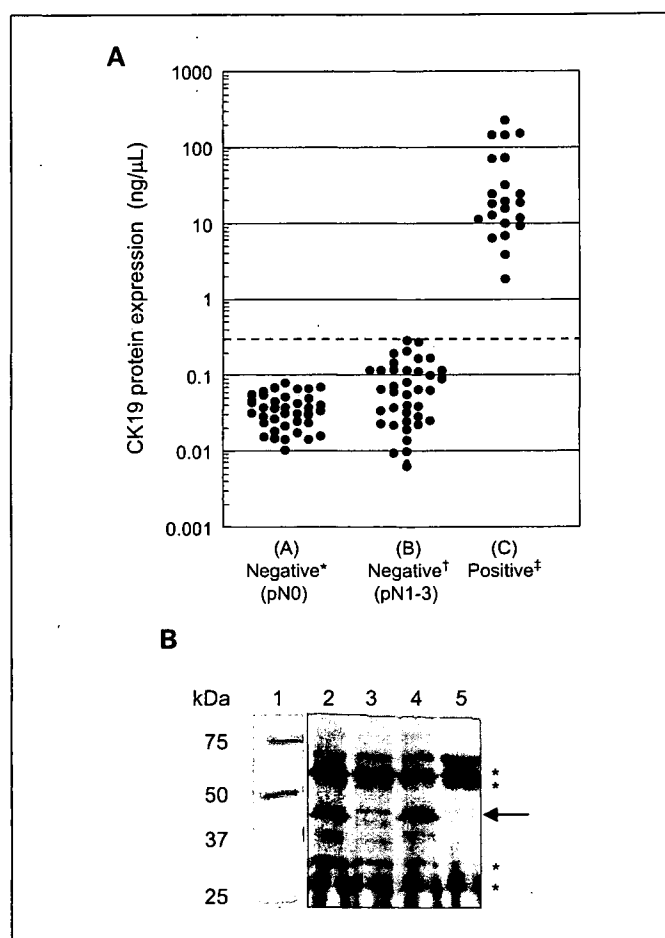

Fig. 5. CK19 protein expression in lymph node lysates. *A,* CK19 protein expression in histopathologically positive and negative lymph node lysates. *, histopathologically negative lymph nodes dissected from pN0 patients. †, histopathologically negative lymph nodes dissected from pN1-3 patients. ‡, histopathologically positive lymph nodes. The CK19 protein expression was determined by Western blot analysis (see Materials and Methods). Broken line, cutoff line between micrometastasis and nonmetastasis. The protein concentration of representative lymph node lysates used in this experiment was within the range of 8.7 to 11.6 μg/μL. *B,* a representative example of Western blot analysis of CK19 protein in lymph node lysates. Lane 1, molecular weight markers stained with Coomassie brilliant blue. Lanes 2 and 4, histopathologically positive lymph node lysate. Lanes 3 and 5, histopathologically negative lymph node lysate. Arrow, CK19 protein. *, nonspecific bands. The vertical scale shows molecular weights.

Fig. 6. Expression of mRNA markers in histopathologically positive and negative lymph nodes. The selected mRNA markers (CK19, FOXA1, SPDEF, CEA, MGB1, TACSTD2, and MUC1) were evaluated by QRT-PCR using 11 histopathologically positive (●) and 15 negative (O) lymph nodes from 26 patients.
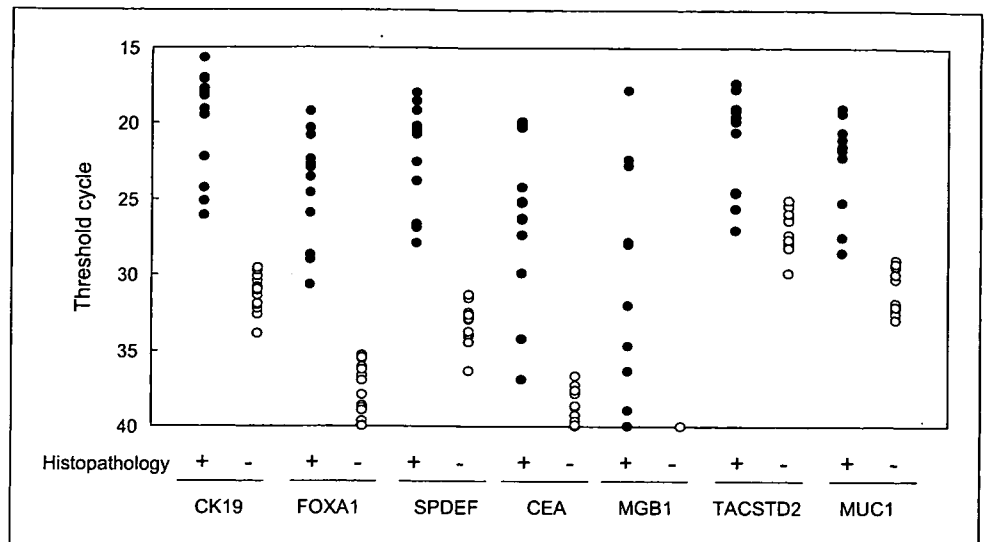
immunohistochemistry-based histopathologies were 86.7% and 91.1%, respectively, based on the results of three-level CK19 immunohistochemistry-based histopathology (Supplementary Table S3).

The concordance rate between the OSNA assay and the CK19 immunohistochemistry-based three-level histopathology for 325 lymph nodes was 98.2%. The concordance rate for SLNs was 96.4%.

No false positive results were found with the OSNA assay of 144 histopathologically negative lymph nodes from 60 pN0 patients, in which neither micrometastasis nor macrometastasis was observed for serial sections from blocks b' and d' (Fig. 3C). Furthermore, the OSNA assay judged 13 ITC cases as negative. These results are summarized in Table 3.

Discordant cases. Six discordant cases were observed between the OSNA assay and CK19 immunohistochemistry-based histopathologic examination (Table 4). Four cases were micrometastasis according to the OSNA assay and were negative according to the CK19 immunohistochemistry-based histopathology. In any case, CK19 mRNA expression of $>10^3$ copies/μL was observed (Table 4). These four discordant cases came from pN1 and pN2 patients. In two of four cases, micrometastasis was observed in the multilevel examinations of blocks b' and d'. On the other hand, two remaining cases (Table 4, *samples 5* and *6*) were negative according to the OSNA assay and micrometastasis according to the three-level histopathology. Samples 5 and 6 showed metastatic foci of 0.3 and 0.4 mm in the long axis, which were observed on surfaces i' and ii', respectively. When i' and ii' were histopathologically examined, about 0.2 mm was shaved from the surfaces of blocks b' and d'. Therefore, the amount of metastatic foci in blocks a' and c' that were used for the OSNA assay (i.e., a' and c') could not be quantified.

We also measured the amount of CK19 protein by Western blot analysis of the lysate used in each discordance case. A cutoff value for CK19 protein expression between metastasis positive and negative lymph node was determined by the distribution of CK19 protein expression in 37 histopathologically negative lymph nodes from 16 pN0 patients. The distribution could be described as a logarithmic normal distribution. The statistical analysis indicated that an average

value +3 SD was 0.13 ng/μL. Based on this analysis, the cutoff value was determined to be 0.3 ng/μL, which is the upper limit of the CK19 protein expression in 54 histopathologically negative lymph nodes from pN1-3 patients (Fig. 5A). Furthermore, CK19 protein expression in 22 histopathologically positive lymph nodes from 10 patients contained protein levels over the cutoff value.

Based on this cutoff value, we measured the amount of CK19 protein using quantitative Western blot analysis of the lysate for the OSNA assay of samples 1, 2, and 5. As described in Table 4, samples 1 and 2 showed an amount of CK19 protein expression equivalent to micrometastasis. Sample 5 exhibited no CK19 protein expression.
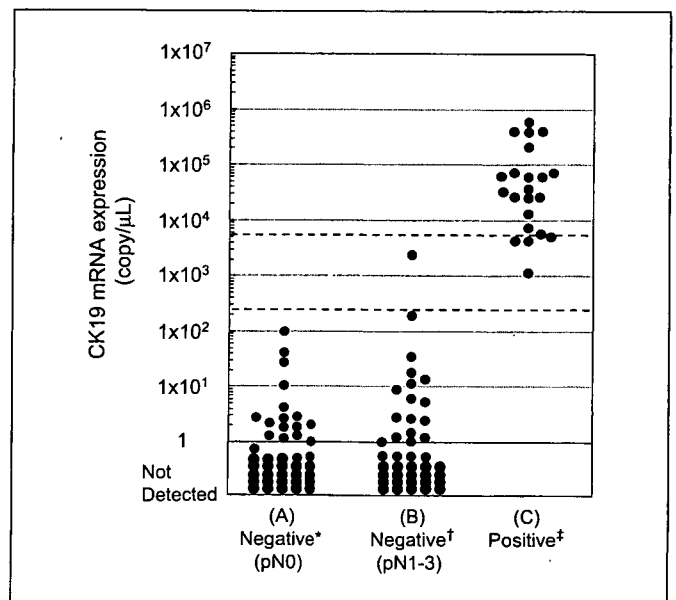

Fig. 7. CK19 mRNA expression in the OSNA assay carried out under the protocol A (Fig. 3 A). *, histopathologically negative lymph nodes dissected from pN0 patients. †, histopathologically negative lymph nodes dissected from pN1-3 patients. ‡, histopathologically positive lymph nodes. Top broken line, cutoff between macrometastasis and micrometastasis. Bottom broken line, cutoff between micrometastasis and nonmetastasis.

Table 3. Comparison of the OSNA assay with the histopathologic examination

Number of lymph nodes	OSNA*	Histopathologic examination [†]			
		Macrometastasis	Micrometastasis	ITC	Negative [‡]
325 from 101 patients	++	34 (34)	0 (0)	0 (0)	0 (0)
	+	6 (5)	3 (1)	0 (0)	4 (0)
	-	0 (0)	2 (2)	13 (11)	263 (0)
81 SLNs from 49 patients	++	11 (11)	0 (0)	0 (0)	0 (0)
	+	1 (0)	2 (1)	0 (0)	1 (0)
	-	0 (0)	2 (2)	3 (2)	61 (0)
144 from 60 pN0 patients	++	0 (0)	0 (0)	0 (0)	0 (0)
	+	0 (0)	0 (0)	0 (0)	0 (0)
	-	0 (0)	0 (0)	3 (3)	141 (0)

*In the OSNA assay, (++), (+), and (-) show >5 × 10^3, 2.5 × 10^2 to 5 × 10^3, and <2.5 × 10^2 copies/μL of CK19 mRNA, respectively.
[†] Histopathologic examinations with H&E and CK19 immunohistochemistry were carried out in all samples. In cases where metastatic foci were observed in the histopathologic examination by either H&E or CK19 immunohistochemistry, the sample was categorized as macrometastasis, micrometastasis, or ITC. The results of the three-level CK19 immunohistochemistry-based histopathologic examination were determined by the consensus of three third-party pathologists. The number of lymph nodes judged to be positive based on the three-level H&E-based histopathologic examination is shown in parenthesis.
[‡] No cancer cells were observed in either the immunohistochemistry- or H&E-based histopathologic examinations.

Discussion

The detection of lymph node metastasis by RT-PCR (37–40) and by QRT-PCR (12, 19–25) has been studied previously. CK19 mRNA has been described as having the highest sensitivity at nearly 90%. However, there are drawbacks using CK19 mRNA due to the concomitant amplification of pseudogenes in genomic DNA that lead to false positive results. For this reason, a combination of two or three markers has been used.

We evaluated 45 potential mRNAs and finally selected CK19 mRNA as the best marker for the OSNA assay. To use CK19 mRNA as a marker, we designed RT-LAMP primers that do not amplify the known CK19 pseudogenes (see Materials and Methods). In addition, the lymph node solubilization step in the OSNA assay was carried out at pH 3.5. At this pH, almost all genomic DNA precipitates out. Even when the sample still contained genomic DNA, DNA amplification is unlikely to occur in the OSNA assay because the RT-LAMP step is carried out at 65°C, a temperature at which genomic DNA typically does not denature. Indeed, purified genomic DNA from metastatic lymph nodes was not amplified in the OSNA assay.

In the present clinical study assessing 325 lymph nodes from 101 patients, an overall concordance rate between the OSNA assay and the CK19 immunohistochemistry-based three-level

histopathology was 98.2%. A concordance rate of 96.4% was obtained with 81 SLNs from 49 patients. On the other hand, 1 of 40 macrometastatic cases and 2 of 5 micrometastatic lymph nodes, as defined by CK19 immunohistochemistry-based histopathology, were missed by H&E-based histopathology. Therefore, the sensitivity of three-level H&E-based histopathology was 93.3% based on the three-level CK19 immunohistochemistry-based histopathology. Furthermore, the sensitivity of one- and two-level CK19 immunohistochemistry-based histopathologies is 86.7% and 91.1%, respectively, based on the three-level CK19 immunohistochemistry-based histopathology (Supplementary Table S3). These results indicate that the performance of the OSNA assay is better than that of one- and two-level CK19 immunohistochemistry-based histopathologies and almost equivalent to three-level CK19 immunohistochemistry-based histopathology.

Chu and Wiess (41) reported that 98.2% of primary breast cancer tissues exhibit CK19 protein expression. Two of our authors (Tsujimoto and Tsuda) also examined the CK19 immunohistochemistry-based histopathologic examination of primary breast cancer tissues and found that there was no CK19 protein expression in 20 (2.2%) of 896 cases examined. However, low CK19 mRNA expression in lymph nodes has not been reported.

Table 4. Discordant cases between the OSNA assay and three-level histopathologic examination

Discordant case	CK19 mRNA (copy/μL)	CK19 protein (ng/μL)*	Histopathologic examination [†]	Nodal status
1	9.6 × 10^2	1.4	Negative	pN2
2	1.5 × 10^3	1.6	Negative	pN1
3	2.3 × 10^3	Not tested	Negative	pN1
4	3.6 × 10^3	Not tested	Negative	pN1
5	ND	0.04	Micrometastasis	pN1
6	ND	Not tested	Micrometastasis	pN1

Abbreviation: ND, not detected.
*Amount of CK19 protein was determined by Western blot analysis (see Materials and Methods).
[†] Results of CK19 immunohistochemistry-based histopathologic examination of the sections i', ii', and iii' of protocol C (Fig. 3C).

In the present clinical study, CK19 immunohistochemistry-based histopathologic examination of two lymph nodes from one patient revealed metastatic foci smaller than macrometastasis despite the presence of macrometastasis defined by H&E-based histopathologic examination; the histologic type of this primary tumor was neuroendocrine carcinoma. These samples unequivocally had low CK19 expression. The OSNA assay of these samples was positive, indicating that CK19 mRNA was expressed despite the low protein expression found by CK19 immunohistochemistry.

In QRT-PCR studies in which several mRNA markers have been used (12, 19, 24, 25), the ability to quantitatively discriminate macrometastasis from micrometastasis has not been discussed. In the OSNA assay, the solubilization of a lymph node is followed by mRNA amplification. Regardless of the size of the lymph node, a constant portion of lysate is transferred to an RT-LAMP reaction. This indicates that the OSNA assay can, in principle, discriminate macrometastasis from micrometastasis and micrometastasis from nonmetastasis when the cutoff values of CK19 mRNA are properly set. To ensure the quantitative capacity of the OSNA assay, endogenous factors should not interfere with the RT-LAMP reaction. We showed that the presence of a lysate obtained from a lymph node (130-600 mg) did not interfere with the OSNA assay (Fig. 1B). A 600-mg sample of lymph node is equivalent to that having a diameter of about 1 cm. The presence of fat or the reagents that were used to identify SLNs, e.g., radioisotope colloid and blue dyes, did not also interfere with the reaction (data not shown).

We observed no false positive result in the OSNA assay from 144 histopathologically negative lymph nodes (60 pN0 patients). In the statistical analysis of the copy numbers of CK19 mRNA in these 144 lymph nodes, the average value of CK19 mRNA expression +3 SD was <2.5 × 10^2 copies/μL, indicating that the probability of negative lymph nodes showing >2.5 × 10^2 copies/μL is low in the OSNA assay. In the OSNA assay, all 13 ITC cases were judged as nonmetastasis (Table 3).

Based on the serial sectioning experiment (Table 1), the average copy numbers equivalent to 0.2^3, 0.3^3, and 0.4^3 mm^3 can be calculated to be 3.9 × 10^1, 1.3 × 10^2, and 3.1 × 10^2 copies/μL, respectively. Therefore, the cutoff value of 2.5 × 10^2 copies/μL in the OSNA assay can theoretically detect metastatic foci of 0.3^3 to 0.4^3 mm^3.

The OSNA assay identified 34 cases of macrometastasis out of 40 macrometastatic lymph nodes defined by the per-manent three-level CK19 immunohistochemistry-based histopathology. The concordance rate was 85.0%. The remaining six cases were identified as micrometastasis. This is the first example of a molecular biological method with the potential to quantify the size of metastatic foci in a lymph node.

Six discordant cases were observed between the OSNA assay and CK19 immunohistochemistry-based histopathologic examination (Table 4). The quantitative Western blot analysis of the discordant cases (samples 1 and 2) clearly showed the presence of an amount of CK19 protein equivalent to micrometastasis. Although the possible presence of benign epithelial cells such as glandular inclusions in the lymph nodes cannot be eliminated, the results may be better explained by the presence of metastatic foci in the lymph nodes in light of the results of the specificity study and the amount of CK19 protein expression. Two other cases (Table 4, samples 5 and 6) were negative according to the OSNA assay, but were judged positive for micrometastasis according to three-level histopathology. These two cases showed metastatic foci of 0.3 and 0.4 mm. Therefore, the amount of metastatic foci in blocks a' and c' used for the OSNA assay cannot be estimated exactly. Indeed, in sample 5, the quantitative Western blot analysis of CK19 protein showed no expression of CK19 protein (Table 4).

The results of the clinical study indicate that using one-half of a lymph node in the OSNA assay gave nearly the same results as the three-level histopathology. It became clear in the clinical study conducted at six facilities that the OSNA assay is rapid enough to be done during surgery. Furthermore, the assay would be convenient and objective compared with the intraoperative immunohistochemistry-based histopathologic examination, which is usually done by an experienced pathologist (42, 43).

Acknowledgments

References

1. Donegan WL. Tumor-related prognostic factors for breast cancer. CA Cancer J Clin 1997;47:28–51.
2. van Diest PJ, Peterse HL, Borgstein PJ, Hoekstra O, Meijer CJ. Pathological investigation of sentinel lymph nodes. Eur J Nucl Med 1999;26:S43–9.
3. Weaver DL, Krag DN, Ashikaga T, Harlow SP, O'Connell M. Pathologic analysis of sentinel and nonsentinel lymph nodes in breast carcinoma: a multicenter study. Cancer 2000;88:1099–107.
4. Sabel MS, Zhang P, Barnwell JM, Winston JS, Hurd TC, Edge SB. Accuracy of sentinel node biopsy in predicting nodal status in patients with breast carcinoma. J Surg Oncol 2001;77:243–6.
5. Stitzenberg KB, Calvo BF, Iacocca MV, et al. Cytokeratin immunohistochemical validation of the sentinel node hypothesis in patients with breast cancer. Am J Clin Pathol 2002;117:729–37.

6. Luini A, Gatti G, Ballardini B, et al. Development of axillary surgery in breast cancer. Ann Oncol 2005;16: 259–62.
7. Cote RJ, Peterson HF, Chaiwun B, et al. Role of immunohistochemical detection of lymph-node metastases in management of breast cancer. International Breast Cancer Study Group. Lancet 1999; 354:896–900.
8. Van Diest PJ, Torrenga H, Borgstein PJ, et al. Reliability of intraoperative frozen section and imprint cytological investigation of sentinel lymph nodes in breast cancer. Histopathology 1999;35:14–8.
9. Torrenga H, Rahusen FD, Meijer S, Borgstein PJ, van Diest PJ. Sentinel node investigation in breast cancer: detailed analysis of the yield from step sectioning and immunohistochemistry. J Clin Pathol 2001; 54:550–2.

10. Lyman GH, Giuliano AE, Somerfield MR, et al. American Society of Clinical Oncology guideline recommendations for sentinel lymph node biopsy in early-stage breast cancer. J Clin Oncol 2005;23:7703–20.
11. Tanis PJ, Boom RP, Koops HS, et al. Frozen section investigation of the sentinel node in malignant melanoma and breast cancer. Ann Surg Oncol 2001;8: 222–6.
12. Hughes SJ, Xi L, Raja S, et al. A rapid, fully automated, molecular-based assay accurately analyzes sentinel lymph nodes for the presence of metastatic breast cancer. Ann Surg 2006;243:389–98.
13. Leidenius MH, Krogerus LA, Toivonen TS, Von Smitten KJ. The feasibility of intraoperative diagnosis of sentinel lymph node metastases in breast cancer. J Surg Oncol 2003;84:68–73.
14. Fortunato L, Amini M, Frrina M, et al. Intraoperative